CellPress

Neuron
Article

Wnt-Fzd Signaling Sensitizes Peripheral Sensory Neurons via Distinct Noncanonical Pathways

Manuela Simonetti,[1,6,*] Nitin Agarwal,[1] Sebastian Stösser,[1] Kiran Kumar Bali,[1,6] Emil Karaulanov,[2] Rashmi Kamble,[1] Blanka Pospisilova,[1] Martina Kurejova,[1] Walter Birchmeier,[3] Christof Niehrs,[2,4] Paul Heppenstall,[5,6] and Rohini Kuner[1,6,*]
[1]Institute for Pharmacology, University of Heidelberg, Im Neuenheimer Feld 366, 69120 Heidelberg, Germany
[2]Institute of Molecular Biology (IMB), Mainz, Germany, Ackermannweg 4, 55128 Mainz, Germany
[3]Max-Delbrück-Center for Molecular Medicine (MDC), Robert-Rössle-Strasse 10, 13092 Berlin-Buch, Germany
[4]Division of Molecular Embryology, DKFZ-ZMBH Alliance, Heidelberg, Im Neuenheimer Feld 280, 69120 Heidelberg, Germany
[5]European Molecular Biology Laboratory, Adriano Buzzati-Traverso Campus, Via Ramarini 32, 00015 Monterotondo, Italy
[6]Molecular Medicine Partnership Unit, Otto Meyerhof Center, Im Neuenheimer Feld, 69120 Heidelberg, Germany
*Correspondence: manuela.simonetti@pharma.uni-heidelberg.de (M.S.), rohini.kuner@pharma.uni-heidelberg.de (R.K.)
http://dx.doi.org/10.1016/j.neuron.2014.05.037

SUMMARY

Wnt signaling represents a highly versatile signaling system, which plays diverse and critical roles in various aspects of neural development. Sensory neurons of the dorsal root ganglia require Wnt signaling for initial cell-fate determination as well as patterning and synapse formation. Here we report that Wnt signaling pathways persist in adult sensory neurons and play a functional role in their sensitization in a pathophysiological context. We observed that Wnt3a recruits the Wnt-calcium signaling pathway and the Wnt planar cell polarity pathway in peripheral nerves to alter pain sensitivity in a modality-specific manner and we elucidated underlying mechanisms. In contrast, biochemical, pharmacological, and genetic studies revealed lack of functional relevance for the classical canonical β-catenin pathway in peripheral sensory neurons in acute modulation of nociception. Finally, this study provides proof-of-concept for a translational potential for Wnt3a-Frizzled3 signaling in alleviating disease-related pain hypersensitivity in cancer-associated pain in vivo.

INTRODUCTION

Wnt proteins are important, evolutionarily conserved mediators of cell-cell communication that govern cell fate and patterning over development (Patapoutian and Reichardt, 2000; Grigoryan et al., 2008). During sensory development, Wnt signaling has been described as a major regulator of early lineage specificity as well as later differentiation and patterning of neurotrophin-3-positive sensory axons of the dorsal root ganglia (DRG) and development of their contacts with motoneurons in the spinal cord (Patapoutian and Reichardt, 2000; Budnik and Salinas, 2011). Furthermore, Wnt signaling in adult organisms modulates tissue regeneration and homeostasis in several organs as well as plasticity and disease pathophysiology in the adult CNS (Yuan et al., 2012; Grigoryan et al., 2008; MacDonald et al., 2009).

The Wnt proteins are family of 19 highly conserved glycoproteins that are glycosylated and palmitoylated prior to tightly regulated secretion into the extracellular milieu (Komiya and Habas, 2008; MacDonald et al., 2009). Wnts can activate the intracellular canonical or β-catenin-dependent pathway, which involves β-catenin-mediated gene regulation, as well as several noncanonical or β-catenin-independent signal transduction cascades, all via activation of cell-surface G protein-coupled receptors (GPCRs) called Frizzleds (Fzds) (Komiya and Habas, 2008). In addition, Wnt signaling pathways can involve coreceptors in a context-dependent manner, such as the low-density lipoprotein-related protein 5 and 6 (LRP5 and LRP6), as well atypical receptor tyrosine kinases, such as Ryk or Ror (Komiya and Habas, 2008; MacDonald et al., 2009).

Here we report that this classical developmental signaling system is also active in adult sensory nerves and modulates sensitivity to nociceptive stimuli and we elucidate the underlying molecular mechanisms and contributions of diverse canonical and noncanonical pathways. Moreover, we provide proof-of-concept for a therapeutic relevance for interfering with Fzd1/3 signaling in alleviating nociceptive hypersensitivity in models of cancer pain in vivo.

RESULTS

Expression of Wnt Signaling Mediators in Adult Peripheral Sensory Neurons

RT-PCR analysis as well as direct RNA sequencing revealed that a majority of components of the Wnt signaling system are expressed in lumbar DRG of adult wild-type mice (Figure 1A; Table S1 available online); these included diverse Fzds (Fzd1 and Fzd3 being most prominent), coreceptors such as LRP5, LRP6, Ryk, and Ror2, as well as signaling proteins, such as Dishevelled isoforms 1–3 (Dvl1, Dvl2, and Dvl3) and β-catenin, indicating representation of both canonical as well as noncanonical branches of Wnt signaling.

In sections of mouse lumbar DRGs, immunoreactivity for anti-Fzd1 and anti-Fzd3 was observed in neurons costained with the neuronal marker, β-tubulin III; coincubation of the corresponding epitope peptides led to loss of staining upon (Figure 1B). Costaining with marker proteins revealed that 18% of Isolectin-B4-positive (IB_4+ve) nociceptive neurons, 21% of small diameter peptidergic nociceptive neurons express Fzd1, and 42% of NF-200-positive large-diameter (nonnociceptive) neurons express Fzd1 (Figures 1C and 1E). In contrast, anti-Fzd3 immunoreactivity was found in about 40% of small diameter Isolectin-B4-positive nociceptive neurons, about 60% of peptidergic nociceptive neurons, and in about 72% of NF-200-positive neurons (Figures 1D and 1E). Heterozygous BAC transgenic mice expressing GFP in the Fzd3 locus verified the specificity of the Fzd3 antibody and further confirmed the expression profile of Fzd3 sensory neurons in adult mouse DRG (Figure 1F). Furthermore, both Fzd3-GFP mice and the Fzd3 antibody revealed that Fzd3 is targeted to peripheral nerves that are PGP9.5-immunoreactive in the paw skin (Figure 1F).

Functional Impact of Activation of Peripheral Wnt Receptors on Pain Sensitivity

To address the functional significance of potential Wnt3a-Fzd1/3-mediated interactions between peripheral tissues and sensory nerves, we applied recombinant Wnt3a or the vehicle (PBS) via intraplantar injection to the hindpaw of naive wild-type mice. Wnt3a-injected animals did not show any signs of spontaneous pain; however, upon plantar application of graded mechanical stimuli (von Frey hairs) to the surface of the injected paw, the frequency of paw withdrawal responses to mechanical stimuli increased in Wnt3a-treated mice, in contrast to vehicle-treated mice (Figure 2A). Treatment with Wnt3a also led to a dose-dependent decrease in the latency of paw withdrawal in response to infrared heat in the plantar test (Figure 2B), indicating thermal hyperalgesia. Both mechanical and thermal hypersensitivity induced by Wnt3a were dose dependent, with doses as low as 100 pg eliciting significant behavioral changes (Figures 2A–2D), but showed highly divergent onset and peak periods after Wnt application (Figures 2C and 2D).

In all of the ensuing pharmacological experiments throughout this study in which Wnt3a-mediated thermal hyperalgesia was tested at 7 hr postinjection, inhibitors of pathways were given continuously over the entire period up to 7 hr after Wnt delivery. Intraplantar pretreatment with NSC668036, a compound that specifically inhibits Dishevelled and thereby abolishes Wnt-mediated signaling (Shan et al., 2005), completely blocked Wnt3a-mediated thermal as well as mechanical hypersensitivity (Figures 2E and 2F), indicating specific, receptor-mediated functions (Figures 2E and 2F). Furthermore, intraplantar injection of neutralizing, function-blocking antibodies against Fzd1 and Fzd3 completely inhibited Wnt3a-induced mechanical hypersensitivity (Figure 2E) but only partially blocked Wnt3a-induced thermal hyperalgesia (Figure 2F), suggesting a contribution of other Fzds or coreceptors.

We utilized a perfused skin-nerve preparation from the mouse hindpaw and performed electrophysiological recordings on single A-delta mechanoceptor fibers in the saphenous nerve in response to graded mechanical stimulation of the innervation territory in the skin (Koltzenburg et al., 1997) (Figure 2G). In contrast to treatment with vehicle, application of Wnt3a to the innervated skin led to a dose-dependent potentiation of nerve responses within 30 min (average responses shown Figure 2H), thereby suggesting that Wnt3a can directly sensitize peripheral sensory nerves. As compared to vehicle, 69% of fibers tested showed more than 20% increase in their response magnitudes, and the remaining 31% did not sensitize (Figure 2I), indicating that only a subpopulation of nociceptors are responsive to Wnt3a.

Minor Contribution of the Canonical Pathway to Wnt3a-Induced Pain Hypersensitivity

To understand the mechanisms, we first addressed the contribution of the classical Wnt canonical β-catenin pathway in sensory neurons, which is one of the best understood of all Wnt signaling pathways (Grigoryan et al., 2008) (Figure 3A). Briefly, interaction of Wnt ligands with Fzd receptors and its coreceptor Lrp6 recruits Dishevelled, induces phosphorylation of Lrp6, and further recruits the Axin complex to the activated receptor, leading to inhibition of β-catenin phosphorylation and thereby to the accumulation of cytosolic β-catenin (Figure 3A). β-catenin then travels to the nucleus to form complexes with TCF/LEF-family transcriptional factors and thereby activate Wnt-target gene expression (MacDonald et al., 2009). By employing three complementary approaches, we observed that Wnt3a stimulates the activation of the canonical pathway in a fraction of DRG neurons. First, in neuron-enriched cultures of mouse DRG, Wnt3a-treatment led to a small, but significant, upregulation of Axin2 and Dkk1 transcripts, which are classical β-catenin transcriptional targets (Glinka et al., 1998) (Figure 3B). Second, immunocytochemistry on cultured DRG neurons revealed that 5% ± 1% of DRG neurons demonstrated a Wnt3a-induced nuclear translocation of β-catenin (Figure 3C), which increased to 20% ± 4% cells when nonneuronal cells were allowed to grow in DRG cultures, suggesting that the canonical pathway may be operational to a more significant extent in nonneuronal cells than in neurons in adult DRG. Finally, in a reporter mouse line in which β-galactosidase expression is driven by activated β-catenin and TCF signaling in vivo (BAT-GAL mice; Maretto et al., 2003), 1% ± 0.3% and 7% ± 1% of DRG neurons showed β-galactosidase activity at 24 hr after intraplantar injection of PBS or Wnt3a, respectively (Figure 3D). Consistent with the reported inhibition of canonical Wnt signaling by noncanonical signaling, in particular via pathways downstream of Ca^{2+}/calmodulin-dependent protein kinase II (CaMKII) activation (Ishitani et al., 2003), 25% ± 5% of DRG neurons showed β-galactosidase activity when we treated mice with intraplantar Wnt3a in the presence of a CaMKIIα inhibitor, KN-93 (Figure 3D). Thus, in DRG neurons, Wnt3a-induced activation of canonical pathway is held in check by concurrent activation of noncanonical calcium signaling in vivo.

Modulators of Wnt signaling, such as Fumagillin and Dkk1 (Niehrs, 2006), differentially modulated Wnt3a-induced mechanical hypersensitivity and thermal hyperalgesia (Figure S1). However, because neither Fumagillin nor Dkk1 modify canonical or noncanonical Wnt signaling exclusively, we generated mice lacking β-catenin either in a nociceptor-specific manner

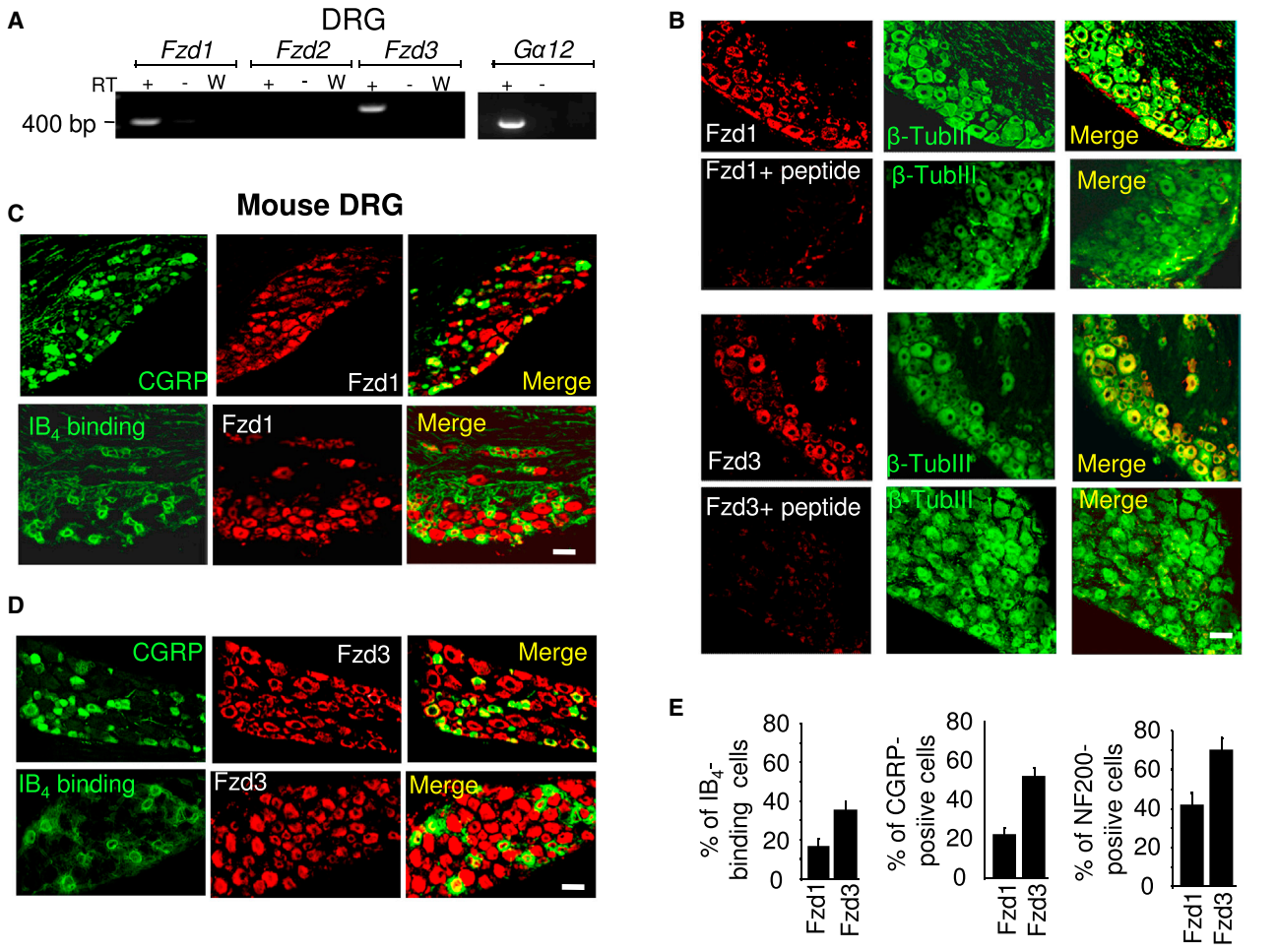

(legend on next page)

(SNS-β-catenin$^{-/-}$ mice; Figures 3E and 3F) generated using SNS-Cre mice (Agarwal et al., 2004) or lacking β-catenin in all cells of the DRG (Adv-β-catenin$^{-/-}$ mice), generated using Advillin-Cre mice (Zurborg et al., 2011) (see scheme of generation and characterization of transgenic mice in Figure S2A). Immunohistochemical analysis confirmed a lack of β-catenin expression in small-diameter neurons in SNS-β-catenin$^{-/-}$ mice and in all DRG neurons in Adv-β-catenin$^{-/-}$ mice but preserved expression in satellite cells in both (Figure S2B). Wnt3a-induced Axin upregulation was completely abolished in the DRG of Adv-β-Catenin$^{-/-}$ mice and partially so in SNS-β-catenin$^{-/-}$ mice (Figure S2C), indicating pan-DRG or nociceptor-specific functional blockade of β-catenin activity, respectively. In behavioral experiments, SNS-β-catenin$^{-/-}$ mice, Adv-β-catenin$^{-/-}$ mice, and their β-catenin$^{loxP/loxP}$ littermates (control) showed comparable magnitudes of mechanical and thermal hypersensitivity upon intraplantar injection of Wnt3a (Figures 3E and 3F). Thus, Wnt3a-induced sensitization was fully intact despite a lack of β-catenin signaling in nociceptors or all DRG neurons.

Furthermore, to avoid any potential occlusion of a behavioral phenotype owing to early postnatal loss of β-catenin expression in the above transgenic mouse lines, we utilized recombinant adeno-associated vectors of serotypes 1 and 2 (rAAV1/2) to deliver Cre recombinase broadly in L3-L4 DRG following direct intra-DRG injections in adult β-catenin$^{loxP/loxP}$ mice in vivo. In other experiments, we employed a newly described, specific modulator of canonical signaling, namely PNU-74654, which inhibits TCF/β-catenin-mediated transcription (Durand et al., 2011; Figure S1C). In both cases, mechanical and thermal hypersensitivity evoked by intraplantar injection of Wnt3a were fully preserved upon adult-onset loss or blockade of β-catenin in DRG neurons, respectively (Figures 3G, 3H, and 3I). Taken together, multiple independent lines of evidence indicate that the contribution of neuronal canonical signaling in the DRG to Wnt3a-induced acute nociceptive hypersensitivity in vivo is relatively minor.

Wnt Signaling via the Noncanonical Calcium Pathway in DRG Neurons: A Mechanistic Basis for Wnt3a-Induced Thermal Hyperalgesia

One of the prominent Wnt noncanonical pathways involves Fzd-G$\alpha_{q/11}$-phospholipase C (PLC-β)-mediated release of calcium from intracellular stores and downstream activation signaling molecules, such as CaMKII, protein kinase C (PKC), Src, and calcineurin, among others (Figure 4A); this pathway is developmentally important, but not commonly operational in all Fzd-expressing cells (Komiya and Habas, 2008). We treated mouse DRG neurons cultured for a few days with Wnt3a or vehicle and performed Fura-2-based calcium imaging. We observed that in contrast to vehicle, approximately 20% ± 3% of DRG neurons treated with Wnt3a responded acutely with slow calcium transients of varying magnitudes, which typically reached peak at 4 ± 2 s after Wnt3a application and had an average duration of 55 ± 18 s. Surprisingly, approximately 39% ± 5% of neurons responded with either a second peak of comparable magnitude or a delayed first peak with a latency of 4–5 min after the application of Wnt3a. To avoid confounding interpretations by growth factors which were added during culturing, we then performed calcium imaging on isolated DRG neurons acutely and applied Wnt3a or vehicle in ringer solution via a continuous perfusion so as to avoid causing any mechanical artifacts. Also under these experimental conditions, we observed results similar to those described above (see Figure 4B for typical examples and a summary graph), indicating that these delayed responses are not mechanical artifacts but probably reflect calcium triggered by mediators that are released from sensory neurons upon Wnt3a signaling. At 3 min after treatment with Wnt3a or vehicle of acutely dissociated DRG neurons that were isolated in the absence of exogenously added growth factors, ELISA-based analysis revealed that Wnt3a-treated cultures showed a significant increase in the concentration of 7 of 12 different cytokines tested, including IL-2, IL-4, IL-10, IL-12, IL-17A, TNFα, and GM-CSF (Figure 4C), several of which are known to activate and sensitize DRG neurons.

Consistent with an activation of the noncanonical Ca^{2+} signaling pathway, neurons in L3/L4 DRGs of mice injected intraplantarly with Wnt3a in the paw showed an increase in immunoreactivity for pCaMKIIα at 30 min after Wnt treatment (Figure 4D) as compared to vehicle-injected mice (Figure 4D). This was further confirmed in western blot analysis (Figures 4E and 4F). Similarly, a marked increase in phosphorylation of another prominent target of calcium, namely Src, was observed at 30 min after Wnt treatment over vehicle-treated mice without changing total Src expression (Figure 4G), which could be blocked upon plantar coinjection of either a pharmacological inhibitor of Src, namely PP2 (Figure S3A), or of an anti-Fzd3 antibody (Figure 4G). Treatment with PP2 or anti-Fzd3 antibody alone did not affect levels of phosphorylated Src (Figure S3).

Both Src and CamKIIα have been associated functionally with sensitization of TRPV1 in sensory neurons and TRPV1 has been shown to be a key mediator of heat hypersensitivity in a wide set of animal models of pain (Zhang et al., 2005, Basbaum et al., 2009). Therefore, we performed several experiments on DRG neurons in vitro and in vivo to determine whether exposure of DRG neurons to Wnt3a quantitatively impacts on the level of expression and surface localization of TRPV1 and characterized the corresponding time course. We utilized a commercial antibody directed against TRPV1 as well as a highly specific

Figure 1. Expression of Wnt Receptors Fzd1 and Fzd3 in Somata and Axons of Peripheral Sensory Neurons

(A) RT-PCR analysis on mouse dorsal root ganglia (DRG). Negative controls: samples without reverse transcriptase (−RT) and water (W); positive control: Gα12 expression.

(B) Immunofluorescence analysis of expression of Fzd1 and Fzd3 in neurons of the lumbar DRG, identified via staining for β-tubulin III (β-TubIII), including controls with corresponding blocking peptides.

(C, D, and E) Immunofluorescence analysis of expression of Fzd1 (C) and Fzd3 (D) in peptidergic (CGRP-positive) and nonpeptidergic (Isolectin-B_4 binding) neurons of mouse lumbar DRG and the corresponding quantification (E).

(F) Use of Fzd3-GFP reporter mice to reveal *Fzd3* promoter-driven GFP expression in sensory and in axons in the paw skin (colocalization with PGP9.5). Scale bars represent 30 μm in (B) and 50 μm in (C), (D), and (F). Data represent mean ± SEM. Also see Tables S1 and S5.

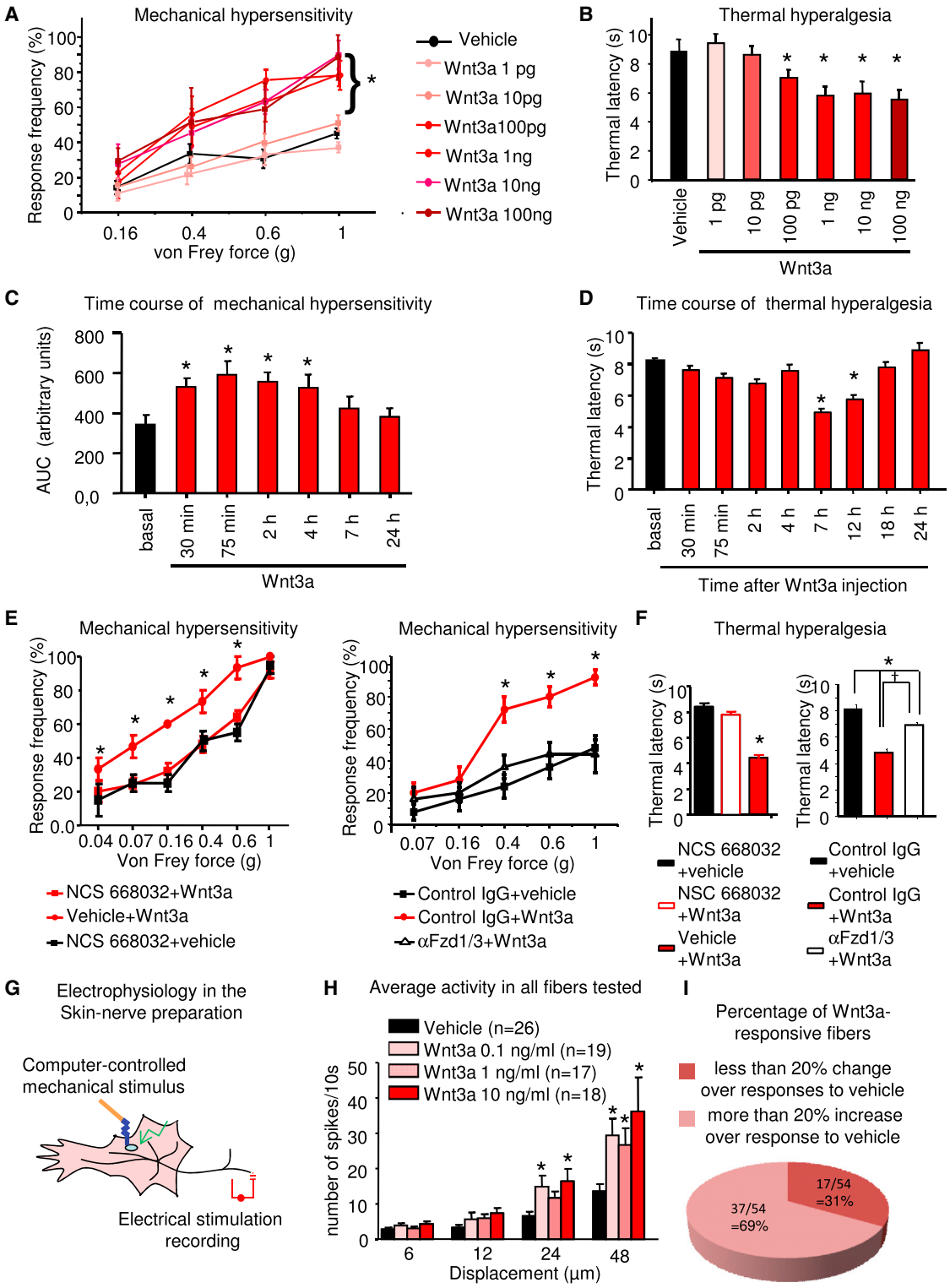

Figure 2. Activation of Wnt3a Receptors in the Skin Leads to Nociceptive Sensitization

(A and B) Characterization and dose-response relationships of the effects of recombinant mouse Wnt3a or of vehicle following a single intraplantar injection in mouse hindpaw on sensitivity to graded mechanical von Frey stimuli (A; expressed as response frequency to five applications/von Frey filament) measured at 30 min postinjection or on thermal sensitivity to infrared red stimuli (B; Hargreaves test) measured at 7 hr postinjection.

(legend continued on next page)

antibody (generously provided by Dr. David Julius, UCSF). Using *Trpv1*$^{-/-}$ mice as a negative control, we observed that the commercial antibody is not specific in immunohistochemistry experiments on DRG sections (data not shown) but is specific in immunocytochemistry experiments on cultured DRG neurons and heterologously expressed TRPV1 (shown in Figures S4A and S4B). Using either of the above antibodies, we observed that after 90 min of Wnt3a exposure, cultured, mature DRG neurons show an increased surface localization of TRPV1 in immunocytochemical staining (an example is shown in Figure S4C). Interestingly, DRG neurons that expressed Fzd3 endogenously showed a prominent immunoreactivity for phosphorylated Src after Wnt3a treatment and demonstrated TRPV1 localization at the cell membrane as compared to a more intracellular distribution in non-Fzd3-expressing cells (Figure 4H). To test quantitative changes in vivo, we ascertained that the specificity of the noncommercial antibody in recognizing the approximate 100 kDa band specific to TRPV1 using DRGs from *Trpv1*$^{-/-}$ mice as a control (an example is shown in Figure S4D). Importantly, in vivo, we observed an increase in the expression of TRPV1 in the membrane fractions derived from L3-L4 DRGs of Wnt3a-injected mice starting only at 4 hr post-Wnt3a injection, and reaching significance only at 6 hr after Wnt injection (example blot and quantitative summary from at least three mice/group is shown in Figure 4I). Finally, upon establishing pulldowns of TRPV1 from distal segments of the sciatic nerve, we observed that an increased expression of TRPV1 in mice receiving intraplantar Wnt3a injections as compared to vehicle-injected mice, at 6 hr, but not at 3 hr, after Wnt3a injection (Figure 4J), which is consistent with the time course of Wnt3a-induced thermal hypersensitivity. This increase in TRPV1 protein expression in the DRG and the sciatic nerve was not reflected in a significant change in *trpv1* mRNA in Wnt3a-treated DRG neurons, indicating that this is not a transcriptionally regulated process (quantitative RT-PCR data in Figure S4E).

In behavioral experiments in vivo, we observed that peripheral blockade of the noncanonical calcium pathway, e.g., using KN-93 to block CaMKIIα and PP2 to block Src activity, led to a complete loss of intraplantar Wnt3a-induced thermal hyperalgesia at 7 hr after Wnt3a injection (bottom panels in Figures 4K and 4L, respectively). In contrast, blockade of neither CaMKIIα nor Src signaling blocked intraplantar Wnt3a-induced mechanical hypersensitivity, measured at 30 min and 2 hr after Wnt3a administration (top panels in Figures 4K and 4L, respectively). In both cases, inhibitors were given continuously over the entire period up to the measurement of thermal hyperalgesia at 7 hr after Wnt delivery.

These data indicate that the calcium arm of Wnt signaling, comprising of calcium-Src-CamKII signaling, directly enhances the membrane localization as well as the peripheral targeting of TRPV1 over a time frame of several hours and thus mechanistically accounts for the delayed onset of Wnt3a-mediated thermal hyperalgesia; however, it does not play a role in Wnt3a-induced mechanical hypersensitivity.

A Key Role for the Planar Cell Polarity Pathway of Wnt Signaling in Peripheral Sensory Neurons

We then explored potential contributions of the planar cell polarity (PCP) arm of Wnt signaling (Figure 5A), in which a Wnt-Fzd interaction brings about activation of Dishevelled-associated activator of morphogenesis 1 (DAAM1) to stimulate the RhoGTPase RhoA and its downstream effector, RhoA-dependent Kinase (ROCK) as well as the RhoGTPase Rac1 and its downstream target, c-Jun amino (N)-terminal kinase (JNK); both RhoA-ROCK and Rac-JNK pathways have diverse cellular targets, including the cellular cytoskeleton (Figure 5A; Komiya and Habas, 2008). Using G-ELISA assays on lysates of neuron-enriched DRG cultures, we observed that exposure to Wnt3a produced a robust activation of the Rac1 in sensory neurons within 15 min (Figure 5B). Accordingly, we observed enhanced JNK phosphorylation in L3-L4 DRGs of mice receiving an intraplantar hindpaw injection of Wnt3a as compared to vehicle-injected mice via immunohistochemistry (typical examples and quantification in Figure 5C) as well as via western blot analysis (examples and quantification in Figure 5D).

In vivo behavioral analyses revealed a key role for some components of the PCP pathway in Wnt3a-mediated mechanical hypersensitivity. A neuron-specific knockdown of Rac1 in L3/L4 DRGs using the AAV virions to express specific, previously validated shRNAs directed against Rac1 led to a loss of Wnt3a-induced mechanical hypersensitivity but a preservation of thermal hyperalgesia as compared to mice expressing scrambled control RNA in the DRG (Figure 5E). Similar results were obtained upon intraplantar pretreatment with an inhibitor of Rac1 (NSC23766; Figure 5F). Furthermore, intraplantar pretreatment with a JNK blocker (SP600125) completely abrogated Wnt3a-induced mechanical hypersensitivity without affecting Wnt3a-induced thermal hyperalgesia (Figure 5G). In contrast, inhibition of ROCK via intraplantar Y-27632 neither affected Wnt3a-induced mechanical hypersensitivity nor thermal hyperalgesia (Figure 5H). These results suggest that the Rac-JNK signaling arm of the PCP pathway, not the RhoA-ROCK arm, contributes to Wnt3a-induced mechanical hypersensitivity.

(C and D) Time-course analyses of the effects of a single intraplantar dose of 10 ng Wnt3a in the mouse hindpaw on sensitivity to graded von Frey stimuli (C) or heat (D).

(E and F) Characterization of effects on mechanical (E) or thermal (F) hypersensitivity elicited by intraplantar Wnt3a (10 ng) by administration of a specific inhibitor of Dishevelled, NSC 668032 (20 ng given 30 min before and 6 hr after Wnt3a injection each) or of neutralizing antibodies against Fzd1 and Fzd3 (2.5 μg each; 1 dose 30 min prior to Wnt3a); vehicle or control IgG served as a negative controls, respectively.

(G, H, and I) Electrophysiological analysis of effects of Wnt3a on activity of identified Aδ-mechanoreceptive fibers in a paw skin-nerve preparation (G); average activity in all recorded fibers upon 60 min exposure to diverse doses of Wnt3a or vehicle (H) and pie diagram revealing the percentage of fibers that responded to Wnt3a (I). y axis in (G) represents responses of mechanosensitive nociceptors to graded mechanical stimuli (represented as displacement of a nanometer in microns on the x axis). *$p < 0.05$ as compared to corresponding vehicle control, two-way ANOVA for random measures followed by post hoc Fischer's test; n = 5–7 mice/group. Data represent mean ± SEM. Also see Figure S1.

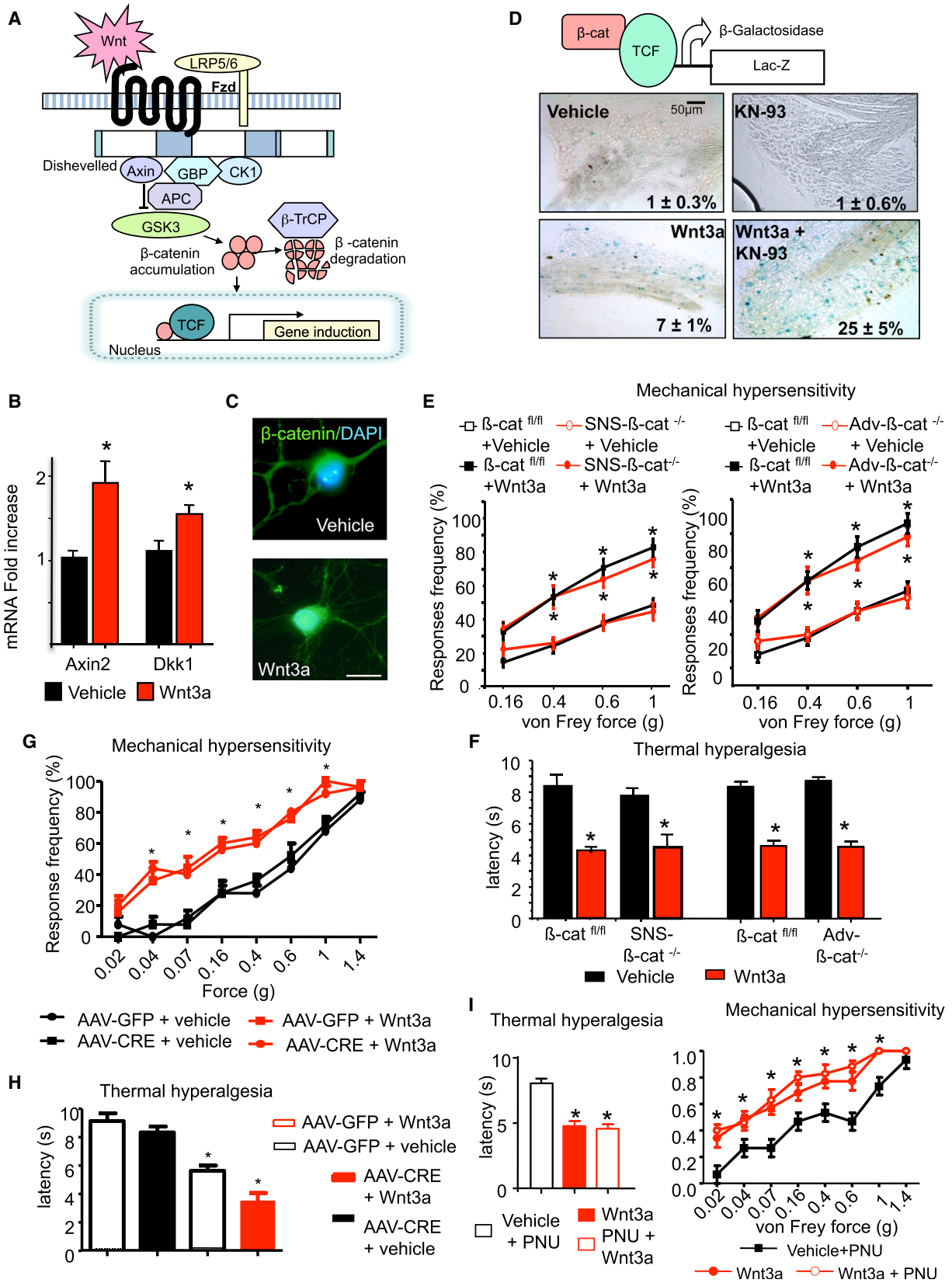

(legend on next page)

Influence of Wnt3a Signaling on Function and Membrane Translocation of TRPA1 and P_2X_3

Based on the above data as well as the observed acute nature of Wnt3a-induced hypersensitivity, we hypothesized that the Wnt-PCP pathway acting via Rac1-JNK leads to rapid modulation of the molecular machinery involved in transducing mechanical pressure in peripheral sensory nerves (Figure 6A). The precise molecular composition of the assembly transducing mechanical touch and pressure into membrane depolarization is not fully clear. However, several mediators have been implicated in mechanical sensitization in peripheral neurons, among which we were interested in the ion channels TRPA1 and P_2X_3 (e.g., Tsuda et al., 2000; Petrus et al., 2007), since we found consensus motifs for JNK phosphorylation in their intracellular segments. To test whether Wnt3a can directly or indirectly modulate P_2X_3 and TRPA1 channels functionally, we employed HEK293 cells heterologously cotransfected with plasmids expressing Fzd3 and either DsRed-tagged P_2X_3 or TRPA1-IRES-YFP and analyzed calcium transients evoked by a first application of Allyl isothiocyanate (AITC; TRPA1 agonist) or α,β-methyleneATP (α,β-meATP, P_2X_3 agonist) as a surrogate parameter for channel activation (example in Figure 6B, top); subsequently, cells were washed and exposed to Wnt3a or vehicle followed by a washout and second application of AITC or α,β-meATP at about 10 min after Wnt3a/vehicle treatment (example in Figure 6B, middle). In contrast to vehicle application, in cells treated with Wnt3a, the second application of α,β-meATP led to calcium transients that were significantly larger in magnitude than those evoked by the first application of the agonist (quantitative summary in Figure 6B, bottom). AITC-induced calcium transients showed a nonsignificant trend for increase within 10 min after Wnt3a application (Figure 6B).

Apart from direct channel modulation, intracellular signaling pathways can regulate ion channels by altering their intracellular trafficking and cell-surface targeting. Indeed, in HEK293 cells coexpressing myc-tagged TRPA1 or myc-tagged P_2X_3 with Fzd3, within 30 min to 1 hr after exposure to Wnt3a, but not vehicle, a marked increase was observed in anti-myc immunoreactivity at the cell surface (Figure 6C). As another independent method of quantitative assessment of Wnt3a-induced membrane translocation of TRPA1 and P_2X_3, we performed surface biotinylation experiments on HEK293 cells transfected with Fzd3 and either myc-tagged TRPA1 or myc-tagged P_2X_3. In contrast to vehicle, HEK293 cells exposed to Wnt3a for 30 min showed a significantly higher content of cell-surface biotin-labeled TRPA1 as well as biotin-labeled P_2X_3 (Figure 6D).

Finally, blockade of peripheral P_2X_3 or TRPA1 via intraplantar injection of A317491 or AP-18 partially, but significantly, blocked mechanical hypersensitivity evoked by peripheral Wnt3a (Figure 6E), while preserving Wnt3a-induced thermal hyperalgesia (Figure S5). Furthermore, intraplantar Wnt3a failed to induce mechanical hypersensitivity in mice genetically lacking TRPA1 (Figure 6E). Thus, the PCP pathway acting via Rac1-JNK enhances the membrane targeting of P_2X_3 or TRPA1 in sensory neurons and can thus account for Wnt3a-induced mechanical hypersensitivity.

Expression Profiles of Mediators of Mechanical versus Thermal Modalities of Wnt3a-Induced Nociceptive Hypersensitivity

Because multiple Fzds show a broad expression over the DRG (Figure 1; Figure S1) and their immediate interaction partners, such as β-catenin, Dishevelled, and G proteins, show ubiquitous expression, we tested the hypothesis that cell-type-specific recruitment of downstream mediators comprising the calcium-Src pathway and PCP-JNK pathway imparts specificity to mechanical and thermal modalities. In immunohistochemistry experiments, we observed that IB4-positive nonpeptidergic nociceptors and NF-200-positive myelinated mechanoreceptive neurons accounted for 86% of neurons showing JNK phosphorylation (Figure S6), indicating a preferential activation of the PCP JNK-Rac pathway in DRG neuron types associated with mechanical hypersensitivity (Cavanaugh et al., 2009). In contrast, CGRP-positive peptidergic nociceptors, which have been associated with thermal hyperalgesia (Cavanaugh et al., 2009), accounted for about 60% of all DRG neurons showing Wnt3a-induced Src phosphorylation, whereas IB4-positive neurons only accounted for 19% of pSrc-positive neurons (Figure S6).

Figure 3. Analysis of Activation of the Wnt Canonical Signaling Pathway in DRG Neurons and Its Contribution to Wnt-Induced Nociceptive Hypersensitivity

(A) Schematic representation of the canonical Wnt signaling pathway.

(B) RT-PCR analysis of Wnt3a-induced increase in the transcription of β-catenin targets in L3-L4 DRG of mice 6 hr after intraplantar injection of Wnt3a (10 ng) or vehicle (n = 5 mice per group).

(C) Example of Wnt3a-induced nuclear translocation of β-catenin in cultured DRG neurons (n = 3 independent culture experiments).

(D) Analysis of Wnt3a-induced β-catenin activation and downstream transcription of β-galactosidase in the DRG of BAT-Gal reporter mice. Shown are representative examples of LacZ staining on sections of DRG from reporter transgenic mice injected intraplantar with vehicle (n = 3), Wnt3a (10 ng; n = 5), KN-93 alone, a blocker of CaMKIIα (0.1 nmol; n = 3), or a combination of Wnt3a (10 ng) and KN-93 (0.1 nmol; n = 5) in the hindpaw. Fraction of LacZ-positive neurons as a function of total number of DRG neurons is given in the insets.

(E and F) No change in intraplantar Wnt3a-induced mechanical hypersensitivity (E) or thermal hyperalgesia (F) in mice genetically lacking β-catenin in a nociceptor-specific manner (SNS-β-catenin$^{-/-}$) as compared to their control littermates (β-catenin$^{fl/fl}$) (n = 10 mice/genotype) or in mice lacking β-catenin in all DRG neurons (Adv-β-catenin$^{-/-}$) as compared to their control littermates (β-catenin$^{fl/fl}$) (n = 8 mice/genotype).

(G and H) Effect of adult-onset neuron-specific deletion of β-catenin via injection of AAV-Cre (or AAV-GFP as control) into L3-L4 DRGs of adult β-catenin$^{fl/fl}$ mice on intraplantar Wnt3a-induced mechanical hypersensitivity (G) and thermal hyperalgesia (H) (n = 8 mice/group).

(I) Effect of specific blockade of β-catenin-dependent transcription with PNU-47654 (PNU, 2 nmol given 30 min before and 6 hr after Wnt3a injection each) on thermal hyperalgesia (left) or mechanical hypersensitivity (right) evoked by a single intraplantar hindpaw injection of Wnt3a (10 ng). *$p < 0.05$ as compared to corresponding vehicle control, two-way ANOVA for random measures followed by post hoc Fischer's test. Scale bars represent 20 μm in (C) and 50 μm in (D). Data represent mean ± SEM. Also see Figures S1 and S2 and Tables S2, S3, and S4.

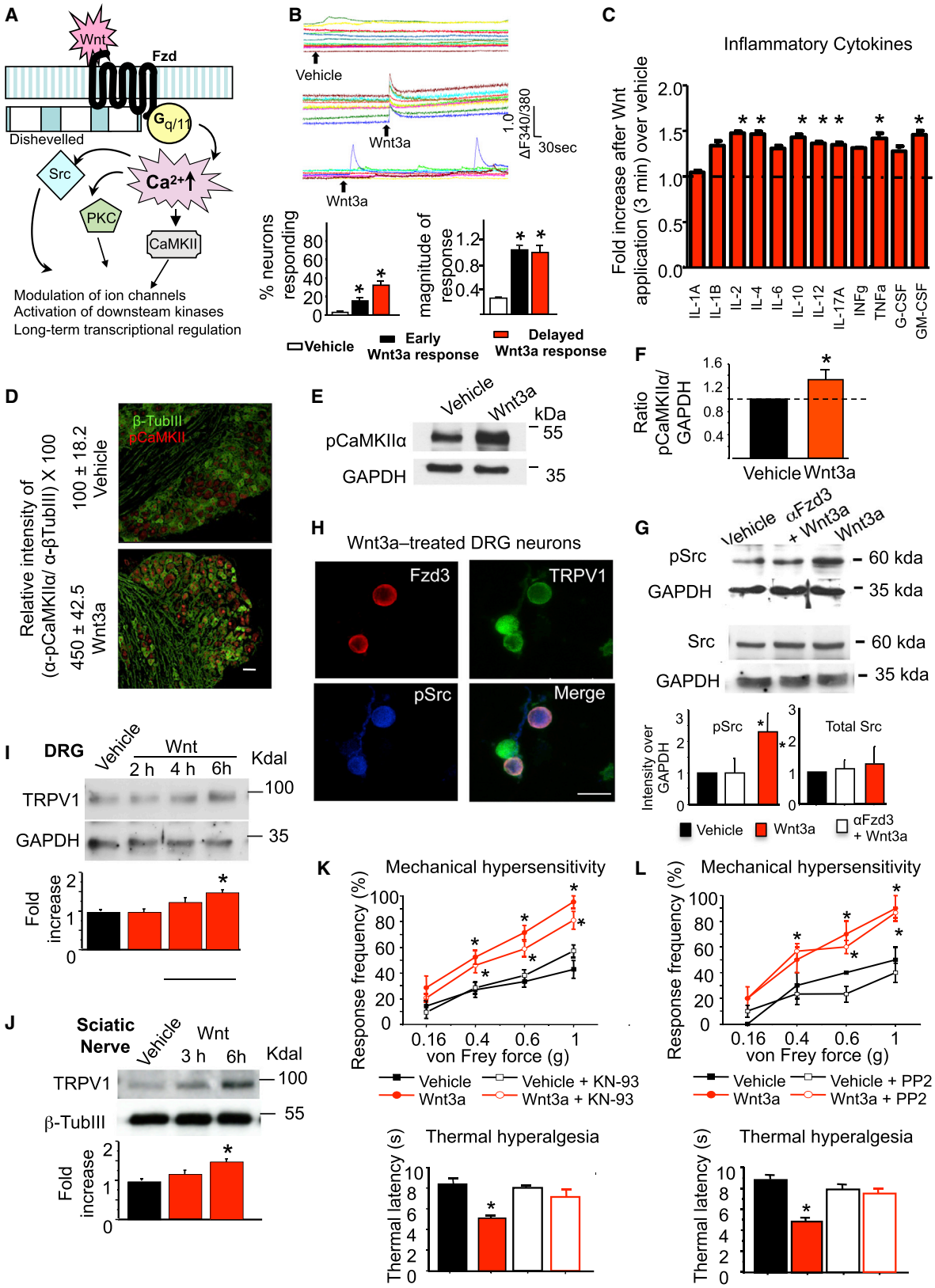

(legend on next page)

Contribution of Wnt3a-Regulated Genes to Subacute to Long-Term Nociceptive Modulation

Wnt signaling can also modulate gene transcription, not only directly via the canonical β-catenin pathway, but also further downstream of noncanonical pathways, such as the calcium signaling pathway. Upon performing a genome-wide transcriptome analysis on neuron-enriched DRG cultures treated with Wnt3a or vehicle for 6 hr, 151 genes were observed to be significantly up- or downregulated in Wnt3a-treated neurons as compared to vehicle-treated neurons (Table S2). These included several genes that have been described in relation to Wnt signaling in other systems or context (Table S3), as well as genes encoding some targets linked to pain modulation previously, such as the chemokine receptor CXCR4 (*Cxcr4*), the receptor tyrosine kinase TrkB (*Ntrk2*), and the proton-gated ion channel Asic3 (*Accn3*). Wnt3a-induced upregulation of *Cxcr4* and *Ntrk2*, but not of *Accn3*, could be confirmed via quantitative real-time PCR analysis on cDNAs from cultured DRG neurons and further validated in DRG samples obtained from mice injected intraplantarly with Wnt3a (Figure S7A). Gene ontology analysis also suggested a role for Wnt3a in regulating expression of some known modulators of nerve activity and synaptic transmission (Table S4).

Furthermore, blocking TrkB via ANA-12 injected intraplantarly three times over 24 hr significantly together with Wnt3a attenuated the thermal as well as mechanical hypersensitivity measured at 24 hr (Figures S7B and S7C). In contrast, blockade of CXCR4 via AMD3100 only attenuated mechanical, but not thermal, hypersensitivity evoked by a 24 hr treatment with Wnt3a (Figures S7B and S7C). These results indicate that Wnt3a-regulated genes can indeed contribute to a subacute modulation of nociception, particularly in pathological states associated with prolonged, high levels of Wnt signals.

Contribution and Translational Potential for Peripheral Wnt Signaling in Disease-Related Pain Hypersensitivity

We then sought to test the biological significance of the above findings in a pathophysiological context involving high peripheral levels of Wnt ligands. Misregulation of Wnt signaling has been causally linked to tumorigenesis, metastasis, osteoporosis, and inflammatory disorders (Fodde and Brabletz, 2007; MacDonald et al., 2009). RT-PCR analysis revealed the expression of Wnt5a, but not of Wnt3a, in the DRGs of naive mice (Figures S8A and S8B), which was confirmed in western blot analysis, using previously characterized antibodies recognizing Wnt ligands (Alfaro et al., 2008) (Figures 7A and 7B; specificity control in Figure S8C). The molecular weights of native Wnt5a and Wnt3a were somewhat smaller than those of recombinant Wnt5a and Wnt3a, which may reflect differences in glycosylation patterns (Komekado et al., 2007) (Figures 7A and 7B). Wnt3a protein was neither detected in the DRG lysates nor in paw skin lysates derived from wild-type naive mice (Figure 7B). In contrast to vehicle-injected mice, mice injected with fibrosarcoma cells into the calcaneous bone of the heel to simulate bone metastases (Cain et al., 2001) or mice injected intraplantarly with complete Freund's adjuvant (CFA) (Hartmann et al., 2004) to induce paw inflammation showed Wnt3a expression in paw lysates, but not in DRG lysates (Figure 7B; Figure S8C); in contrast, Wnt5a expression was evident in DRG lysates, but not in paw lysates, derived from control mice as well as tumor-bearing or inflamed mice (Figure 7A). Thus, tumor growth, and paw inflammation to a lesser extent, is associated with a peripheral availability of Wnt3a in mice.

To test the translational significance of these findings, we studied mechanical hypersensitivity, which develops after implantation of osteolytic fibrosarcoma cells into the calcaneous bone cavity in wild-type mice of the C3H strain (Cain et al., 2001). In this model, we administered soluble Fzd-binding proteins 2 and 3 (sFRPs), which dose dependently bind and sequester all Wnt family ligands (Kawano and Kypta, 2003), or bovine serum albumin (BSA) as a control protein, in the vicinity of the calcaneous bone. In sFRP-treated mice, tumor-induced mechanical hypersensitivity to normally innocuous stimuli, e.g., 0.07 g and 0.16 g, was markedly reduced as compared to BSA-injected mice (Figure 7D). To determine which source of Wnt mediates

Figure 4. Analysis of the Wnt Noncanonical Calcium Signaling Pathway in DRG Neurons and Contribution to Wnt-Induced Nociceptive Hypersensitivity

(A) Schematic representation of the Wnt noncanonical calcium signaling pathway.

(B) Typical examples and quantitative representation of ratiometric Fura2 imaging of rapid and delayed calcium transients evoked upon acute exposure to Wnt3a (200 ng/ml) in comparison to vehicle application in dissociated DRG neurons kept in culture for 16–24 hr in the absence of exogenous growth factors; effects observed immediately as well as 3–5 min after Wnt3a/vehicle application are summarized in the bottom panel; n = 185 neurons over 7 independent experiments, including measures taken to rule out mechanical artifacts.

(C) ELISA-based analysis of release of inflammatory cytokines from cultured mouse DRG neurons upon Wnt3a application (100 ng/ml 3min) or vehicle.

(D, E, and F) Analysis of phosphorylation of CaMKIIα (pCaMKIIα) in L3-L4 DRGs of mice with intraplantar hindpaw injection of Wnt3a (10 ng) or vehicle via immunofluorescence on DRG sections (D) or quantitative western blot analysis (E and F). The numbers on the left side of immunofluorescence panels in (D) represent measurements of intensity of pCaMKIIα signals normalized to β-tubulin signal intensity in the same section (n = 3 mice/group). Panel (F) represents densitometric quantification of pCaMKIIα signals normalized to corresponding GAPDH signals (loading control) from four independent blots.

(G) Western blot analysis of Src-kinase and phosphorylation of Src (pSrc) in L3-L4 DRGs of mice with intraplantar hindpaw injection of vehicle or Wnt3a (10 ng) or Wnt3a (10 ng) in combination with a function-blocking antibody against Fzd3 (4 μg). Densitometric quantifications of pSrc signals or total Src signals normalized to corresponding GAPDH signals (loading control) from five independent blots are shown in the bottom panels.

(H) Example of immunofluorescence on cultured DRG neurons treated with Wnt3a (100 ng/ml) showing a stronger membrane localization of TRPV1 signal only in neurons expressing Fzd3 receptor and activated Src kinase.

(I and J) Examples and densitometric quantifications of western blot analysis of TRPV1 signal in membrane preparation of L3-L4 DRGs (I) or sciatic nerve tissue (J) after intraplantar injection of vehicle or Wnt3a (10 ng) at different time points indicated.

(K and L) Effects of blockade of CaMKIIα (KN-93; 0.1 nmol given 30 min prior to Wnt3a; J; n = 5 mice/group) or Src (PP2; 20 ng given 30 min prior to Wnt3a; K; n = 6 mice/group) in vivo via intraplantar injection on mechanical hypersensitivity (top) and thermal hyperalgesia (bottom) evoked by a single intraplantar hindpaw injection of Wnt3a (10 ng) in comparison to vehicle. In all panels, *$p < 0.05$ as compared to vehicle, two-way ANOVA for random measures followed by post hoc Fisher's test. Scale bars represent 50 μm in (C). Data represent mean ± SEM. Also see Figures S3, S4, and S6.

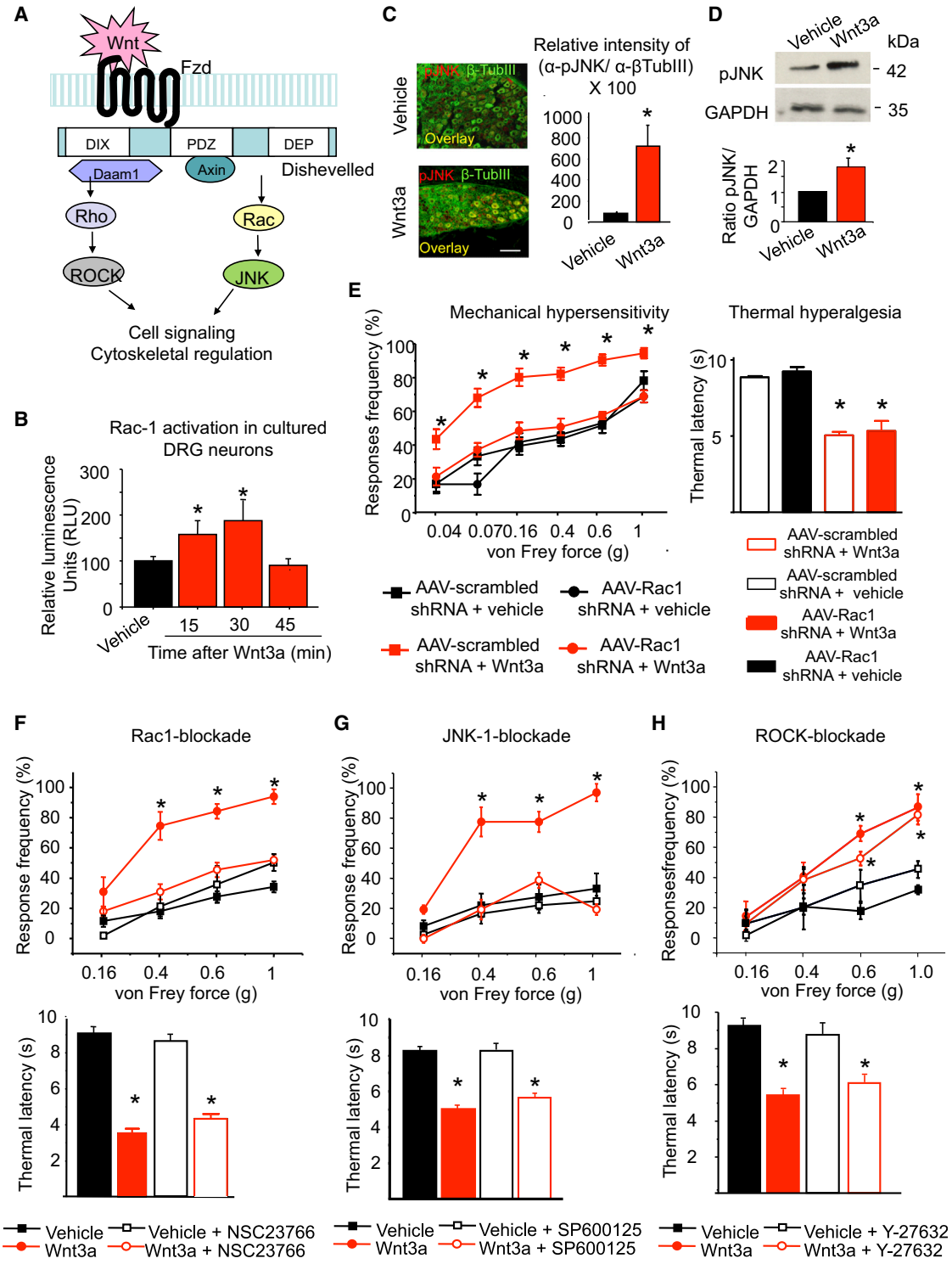

Figure 5. Analysis of Activation of Wnt Noncanonical Planar Cell Polarity Signaling Pathway in DRG Neurons and Its Contribution to Wnt3a-Induced Nociceptive Hypersensitivity

(A) Schematic representation of the Wnt noncanonical PCP pathway.

(B) ELISA-based analysis of Rac1 activation in cultured mouse DRG neurons upon exposure to Wnt3a (200 ng/ml; n = 4 independent culture experiments).

(C) Analysis of phosphorylation of JNK (pJNK) by immunofluorescence in L3-L4 DRGs of mice with intraplantar hindpaw injection of Wnt3a (10 ng) or vehicle (left). Right: measurements of intensity of pJNK signals normalized to β-tubulin signal intensity in the same section (n = 3 mice/group).

(legend continued on next page)

this sensitization in the tumor-pain model in vivo, we administered specific neutralizing antibodies against Wnt3a or Wnt5a or the control IgG in the vicinity of the calcaneous bone over the entire course of tumor growth. Consistent with our expression data (Figures 7A and 7B), we observed that a Wnt3a-neutralizing antibody, but not a Wnt5a-neutralizing antibody or IgG, significantly attenuated tumor-induced mechanical hypersensitivity (Figure 7D).

We then injected mice intraplantarly with a combination of anti-Fzd1 and anti-Fzd3 blocking antibodies (0.2 mg/ml each injected in 25 μl volume) or the corresponding IgG control in the vicinity of the tumor on days 0, 1, 3, 5, and 7 after implantation of tumor cells (Figure 7E). Tumor-bearing mice injected with anti-Fzd1/3 antibodies developed a significantly lower magnitude of tumor-associated hypersensitivity to graded mechanical stimuli than tumor-bearing mice injected with control IgG (Figure 7E). To further address mechanisms, we utilized TRPA1$^{-/-}$ mice, which necessitated employing a model with tumor cells isogenic to the background of the knockout mice, namely lung carcinoma cells (LL2) injected in the paw (Stösser et al., 2010). Tumor-induced mechanical hypersensitivity to mild (0.07 g or 0.16 g) as well as noxious mechanical forces was significantly reduced in TRPA1$^{-/-}$ mice (Figure 7F), indicating a contribution of TRPA1 toward tumor-associated pain. Blockade of P_2X_3, the other Wnt3a target found in our study, has been already reported to alleviate cancer-associated hypersensitivity (Kaan et al., 2010).

Specific Functional Contribution of Fzd3 Expressed in Sensory Neurons toward Tumor-Associated Pain Hypersensitivity

Because the above tools could have potentially affected tumor cells or immune cells in the tumor milieu rather than selectively affecting sensory nerves, we employed lentivirions expressing shRNA against Fzd3 to directly and specifically manipulate Fzd3 signaling in the DRG, which we have previously described (Schweizerhof et al., 2009) (Figure 8A). At 3 weeks after intra-DRG lentiviral injection, marked knockdown of Fzd3 was observed in the L3-L4 DRGs of the Fzd3 shRNA group as compared to the scrambled shRNA group in western blot analysis (Figure 8B) and immunohistochemistry (Figure S8D). Mechanical hypersensitivity evoked by a single intraplantar injection of Wnt3a was strongly and significantly attenuated in mice expressing lentiviral Fzd3 shRNA, but not in mice expressing scrambled shRNA, thereby demonstrating efficacy of Fzd3 knockdown (Figure 8C). Because lentiviral knockdown of Fzd3 may have affected neuronal and nonneuronal cells in the DRG, we also utilized AAV serotypes that yield broad and neuron-specific expression (Figure 8D; absence of colocalization of AAV-GFP with markers for blood vessels, satellite cells, and Schwann cells in DRG) to induce a neuron-specific knockdown of Fzd3 via expression of shRNA (AAV-Fzd3 shRNA; AAV-scrambled shRNA was used as a control). The efficiency of knockdown was verified via western blotting (Figure 8E) as well as immunohistochemistry for Fzd3 (Figure S8E). Behavioral analyses of Wnt3a-induced acute nociceptive hypersensitivity revealed a qualitatively similar phenotype in mice AAV-induced knockdown of Fzd3 as observed in mice with lentivirally induced knockdown of Fzd3 and (Figure 8F; Figure S8D), the magnitude of the phenotype being larger in AAV-treated than in lentivirus-treated mice, since a broader set of neurons were affected. Importantly, the neuron-specific nature of this manipulation ruled out contributions of nonneuronal cells to phenotypic alterations.

Finally, the progressive development of tumor-associated mechanical hypersensitivity was markedly attenuated in mice injected with AAV-Fzd3 shRNA or lentiviral Fzd3 shRNA, but not in control mice injected with AAV scrambled shRNA or lentiviral scrambled shRNA (Figures 8G and 8H; Figures S8F and S8G). Importantly, differences in mechanical hypersensitivity in all of the above groups did not come about owing to major differences in tumor growth per se; gross histopathological analyses of tumor size did not reveal significant differences in the groups tested (Figure 8I).

DISCUSSION

The recent years have witnessed a remarkable extension of the focus on Wnt signaling from its role in development to disease in adult life. For example, Wnt pathway functions in neural circuit development are now providing a basis for developing therapeutic approaches for nerve regeneration and circuit repair after injury or disease (MacDonald et al., 2009; Budnik and Salinas 2011). The present study now provides evidence that components of this developmentally active system are retained in adult dorsal root ganglia and play a key role in modulating sensitivity of peripheral axons to mechanical and thermal sensory stimuli.

In the Wnt signaling system, the rich diversity of Wnt ligands is mirrored by an intriguing complexity of receptors, coreceptors, and signaling effectors. Here, we focused on Fzd3 and Fzd1 as key receptors on sensory nerves on the basis of our expression analyses as well as observations that blocking Fzd1 and Fzd3 function or knocking down the expression of Fzd3 alone specifically in DRG neurons nearly abrogated Wnt-induced hypersensitivity. Whereas Wnt5a was found to be expressed in the DRG and may thus function in an autocrine manner, Wnt3a emerged as a ligand that is abundant in peripheral tissues in a pathological context only, such as upon inflammation or

(D) Western blot analysis of phosphorylation of JNK in L3-L4 DRGs of mice with intraplantar hindpaw injection of vehicle or Wnt3a (10 ng). Densitometric quantification of pJNK signals normalized to corresponding GAPDH signals (loading control) from three independent blots is shown.

(E) Effects of neuron-specific knockdown of Rac1 in L3-L3 DRGs by short-hairpin RNAs (shRNAs) transduced via in vivo DRG injection of recombinant AAV1/2 virions expressing Rac1-specific shRNA or scrambled shRNA (control) on mechanical hypersensitivity (left) and thermal hyperalgesia (right) evoked by a single intraplantar hindpaw injection of Wnt3a (10 ng) in comparison to vehicle.

(F, G, and H) Effects of intraplantar injection of specific inhibitors of Rac1 (NSC23766; 20 μg; F) or JNK (SP600125, 5 μg; G) or RhoA-dependent Kinase (ROCK)(Y-27632; 25 μg; H), each given 30 min before and 6 hr after Wnt3a injection, on mechanical hypersensitivity (top) and thermal hyperalgesia (bottom) evoked by a single intraplantar hindpaw injection of Wnt3a (10 ng) in comparison to vehicle; n = 6 mice/group in all panels. In all panels, *$p < 0.05$ as compared to vehicle, two-way ANOVA for random measures followed by post hoc Fisher's test. Scale bars represent 50 μm in (D). Data represent mean ± SEM. See also Figure S6.

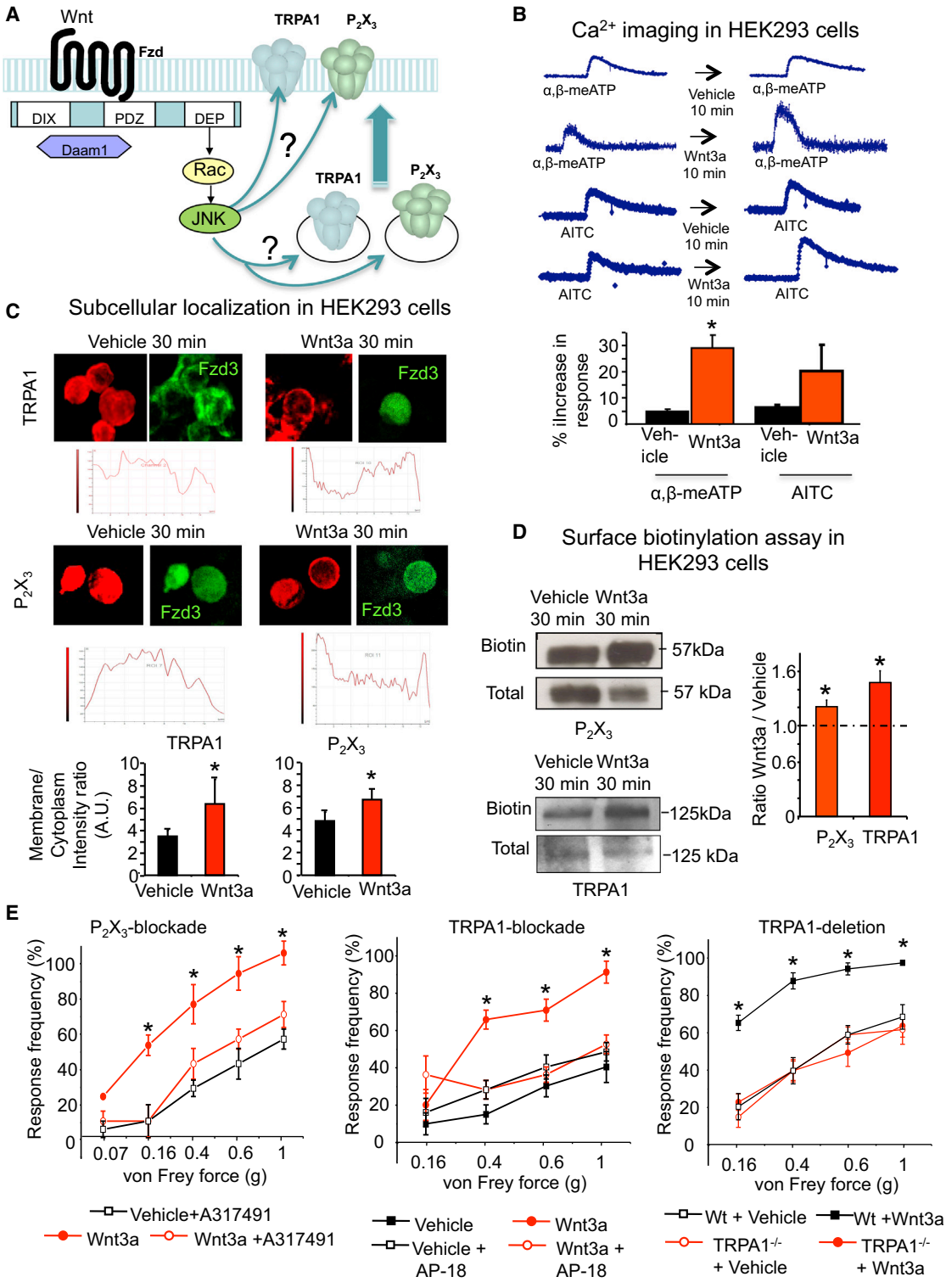

Figure 6. Analysis of Modulation of TRPA1 and P2X3 Function and Localization by Wnt3a Signaling

(A) Schematic representation of potential modulation of ion channels involved in mechanical sensitization by the Wnt noncanonical PCP pathway.

(B) Wnt3a-induced modulation of calcium transients evoked in HEK293 cells by AITC (TRPA1 agonist, 50 μM; n = 3 independent culture experiments) or α,β-meATP (P_2X_3 agonist, 10 μM; n = 4 independent culture experiments). Shown are examples and quantitative summary of transients evoked by two consecutive applications of each agonist separated by an intermittent application of Wnt3a (200 ng/ml) or vehicle.

(legend continued on next page)

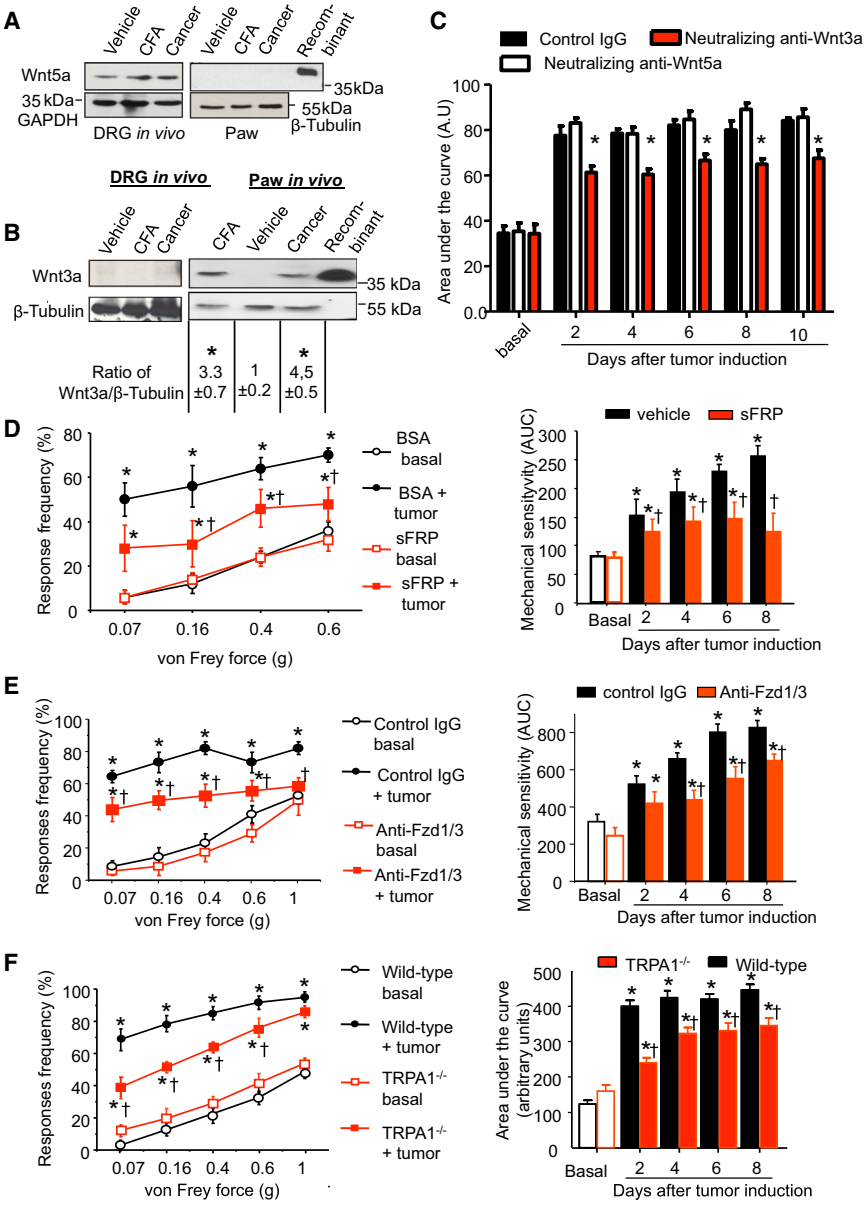

Figure 7. Attenuation of Disease-Associated Pain Hypersensitivity by Pharmacological Intervention in Peripheral Wnt Signaling

(A and B) Expression of Wnt5a (A) or Wnt3a (B) in lysates from hindpaws or DRGs of mice injected intraplantar with vehicle (PBS), complete Freund's adjuvant (CFA), or osteolytic fibrosarcoma cells in the calcaneous bone (cancer). Positive control: recombinant mouse Wnt3a or Wnt5a; loading control: β-tubulin or GAPDH. Numbers in (B) represent densitometric quantification (arbitrary units) of Wnt3a signals normalized to corresponding β-TubIII signals (loading control) from three independent blots.

(C) In the same model, effects of injections of neutralizing antibodies against Wnt3a, Wnt5a or control IgG (4 μg each) in the tumor vicinity on days 1, 3, 5, 7, and 9 on tumor-induced mechanical hypersensitivity; n = 8 mice/group.

(D) In the same model, effects of injection of a mix of soluble Frizzled Binding Proteins 2 and 3 (sFRPs, 100 μg total) or of BSA (100 μg; control) in the tumor vicinity on days 1, 3, 5, and 7 significantly on mechanical hypersensitivity. Left: responses to graded mechanical von Frey stimuli on day 8 after tumor cell implantation. Integral of response frequency-von Frey stimulus intensity curves over the temporal course of tumor progression are shown on the right.

(E) Effects of injection of anti-Fzd1 and anti-Fzd3 function blocking antibodies (4 μg each) or control IgG injections (8 μg) in the tumor vicinity on days 1, 3, 5, and 7 after tumor cell implantation on hypersensitivity to graded mechanical von Frey hairs on day 6 posttumor implantation (left) or over the course of tumor progression (right).

(F) Behavioral analysis of mechanical hypersensitivity in a cancer pain model based on hindpaw subcutaneous injection of isogenic lung carcinoma cells in TRPA1$^{-/-}$ mice and wild-type mice prior to (basal, unfilled symbols) and on day 4 after tumor cell implantation (filled symbols). Integral of response frequency-von Frey stimulus intensity curves over the course of tumor progression are shown on the right. In all panels, n = 7–10 mice/group; *p < 0.05 as compared to baseline values and †p < 0.05 as compared to the corresponding control group (i.e., wild-type mice, IgG or BSA injection); two-way ANOVA followed by post hoc Fischer's test. Data represent mean ± SEM. See also Figure S8.

tumor growth, thereby possessing the capacity for paracrine modulation of neighboring nociceptive nerves and eliciting pain hypersensitivity.

Interestingly downstream of Fzd3/Fzd1, we found evidence for an intriguing dichotomy of noncanonical signaling pathways in mediating mechanical and thermal hypersensitivity. Recent

(C) Wnt3a-induced changes in subcellular localization of myc-tagged TRPA1 or myc-tagged P_2X_3 in HEK293 cells. Shown are typical examples, line profiles on confocal images, and quantification of fluorescence intensity at the cell membrane relative to cytoplasmic localization (n = 40–45 cells/group).

(D) Surface biotinylation assays addressing surface expression of TRPA1 or P_2X_3 in HEK293 cells exposed to vehicle or Wnt3a (200 ng/ml). Shown are typical examples of surface-labeled (biotinylated) TRPA1 or P_2X_3 and their corresponding total input levels (top) and quantification of percentage of increase in Wnt3a-treated cells over vehicle-treated cells of the ratio of biotinylated to total protein (n = 4 and 3 independent experiments for TRPA1 and P_2X_3, respectively).

(E) Effects of blockade of P_2X_3 (A317491, 100 μg; Sigma) or TRPA1 (AP-18, 20 nmol; Sigma), each given 30 min prior to Wnt3a injection, in vivo via intraplantar injection on mechanical hypersensitivity evoked by a single intraplantar hindpaw injection of Wnt3a (10 ng/20 μl) in comparison to vehicle (n = 6 mice for A317491 and vehicle groups each, n = 7 mice for AP-18 and vehicle groups each). Wnt3a-induced mechanical hypersensitivity is abrogated in TRPA1$^{-/-}$ mice, in contrast to their wild-type controls (B6.129PF-2/j strain) (panel at the far right; n = 4–6 mice/group). In all panels, *p < 0.05 as compared to vehicle, two-way ANOVA for random measures followed by post hoc Fisher's test. Data represent mean ± SEM. See also Figure S5.

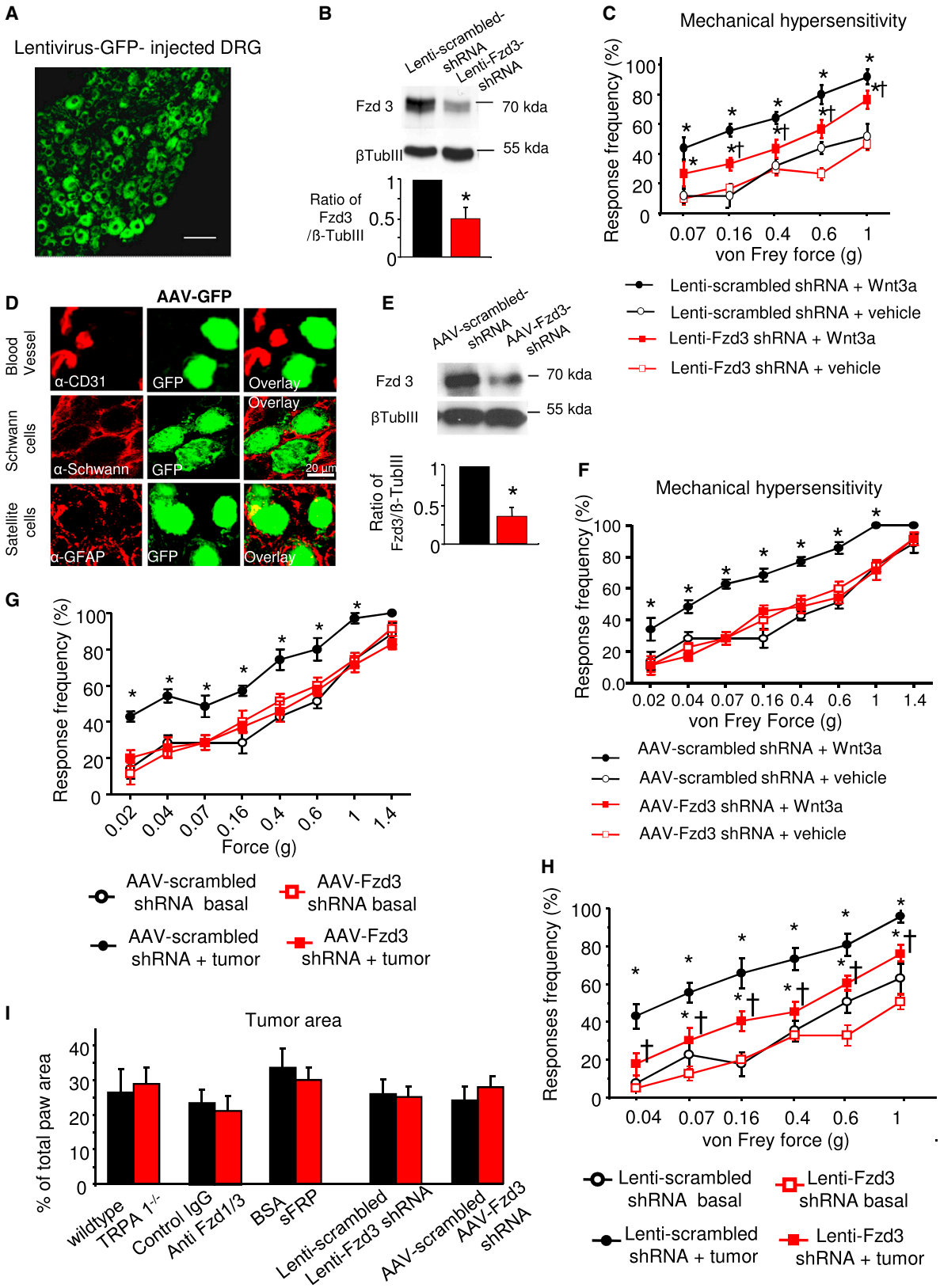

(legend on next page)

advances in understanding Wnt signaling indicate that the same Wnt ligand can activate different signaling pathways depending on the regional and situational context and recent findings show that the receptor context and availability, not the ligand, dictates the Wnt signaling output (Mikels and Nusse, 2006). As such, the PCP pathway acting via Rac-mediated JNK activation, which has so far been primarily associated with Wnt-induced cytoskeletal regulation and thereby in structural modulation in developing central neurons (Budnik and Salinas 2011), was found to be critical for Wnt-induced peripheral mechanical hypersensitivity.

In contrast, diverse cellular assays and in vivo pharmacological and genetic analyses indicate that Wnt3a-induced thermal hypersensitivity is largely mediated by the noncanonical calcium pathway acting via CaMKIIα and Src. Indeed, Src-mediated trafficking of the heat- and proton-sensitive cation channel, TRPV1, from cytoplasmic pools to the cell membrane has been reported to thermal hyperalgesia in response to other sensitizing molecules, including the nerve growth factor (Zhang et al., 2005; Basbaum et al., 2009). Here, we observed that Wnt3a-induced enhanced Src activity is associated with TRPV1 targeting to membrane and terminal compartments of sensory neurons, which requires several hours to unfold, explaining thereby the delayed onset of Wnt3a-induced thermal hyperalgesia.

Our results indicate that the dichotomy of pathways mediating thermal and mechanical hypersensitivity is linked to the type of sensory neurons they are recruited in following Wnt3a-mediated Fzd activation. In particular, the IB_4-binding nociceptors, which have been associated with mechanical nociception by Cavanaugh et al. (2009), and NF-200 positive, which are mechanosensitive populations, showed a dominant recruitment of the Rac-JNK PCP pathway, whereas peptidergic nociceptors, which have been linked to thermal nociception and largely account for the restricted adult expression pattern of TRPV1 (Cavanaugh et al., 2009), showed a preferential recruitment of the Src-TRPV1 signaling pathway. Coupling between Fzds and their signaling mediators occurs in specific microdomains, which can be distinct between different types of sensory neurons, and can thus explain how different pathways can bring about modulation of specific modalities despite the same Wnt-Fzd receptors being activated across all neurons.

The canonical arm of Wnt signaling has been reported to play significant roles over the early stages of DRG development (Patapoutian and Reichardt, 2000). A report published while this study was under review demonstrated that Wnt signaling via the canonical β-catenin pathway in the spinal cord plays a role in neuropathic pain via modulation of NMDA receptors and cytokine release (Zhang et al., 2013). Surprisingly, however, our extensive analysis with pharmacological inhibitors as well as highly specific genetic and shRNA tools did not indicate any functional evidence for the canonical Wnt-signaling pathway in Wnt3a-induced sensitization of peripheral neurons in an acute to subacute context; this was entirely consistent with the small number of DRG neurons showing nuclear translocation of β-catenin in vitro or β-catenin-dependent β-galactosidase induction in highly sensitive reporter mice in vivo as well as the low magnitude of fold regulation of β-catenin-dependent genes in profiling experiments. However, our data do not rule out a role for β-catenin signaling in sensory neurons in a different context, e.g., during regeneration and repair.

Finally, our observations on a sensitizing role for peripheral Wnt signaling and the detailed characterization of neurobiological mechanisms thereof in adult DRG sensory neurons were further consolidated in vivo and placed in translational context, namely in cell-cell communication between adult sensory nerves and tumor cells in cancer states, which constitutes a hallmark mechanistic feature of cancer-associated pain. Given that a DRG-specific knockdown of Fzd3 attenuated tumor-induced mechanical hypersensitivity, using either lentivirions or AAV virions, which enable select knockdown in neurons without affecting Schwann cells, satellite cells, and blood vessels, to the same extent as peripheral inhibition of Fzd1/3 or sequestration of Wnt ligands in the paw, we conclude that Fzd-mediated signaling specifically in sensory neurons plays a key role. Moreover, the finding that sequestering Wnt3a peripherally in the tumor milieu via neutralizing antibodies or soluble Fzds is effective in alleviating tumor-associated mechanical allodynia highlights the translational value of Wnt-Fzd interactions in chronic pain.

In summary, this study places the classical, developmentally critical Wnt signaling system as a key player in the modulation of sensitivity of adult sensory neurons and their peripheral axons. We infer that this peripheral role for Wnt signaling involves an

Figure 8. Evidence for a Functional Role for Neuronally Expressed Fzd3 in the DRG in Cancer-Associated Pain Hypersensitivity

(A) Evidence for lentiviral gene delivery (here, GFP) to sensory neurons following injections into L3-L4 DRGs in mice in vivo.

(B) Evidence for marked knockdown of Fzd3 expression upon injection of lentiviral-Fzd3 shRNA as compared to injection of lentiviral scrambled shRNA in the DRG via western blot analysis using β-Tubulin-III expression as a control; densitometric quantification of three independent experiments is shown on the bottom.

(C) Significant, but partial, blockade of Wnt3a-induced mechanical hypersensitivity in mice with DRG injections of lentiviral Fzd3 shRNA as compared to mice injected with lentiviral scrambled shRNA (n = 6 mice/group).

(D) Evidence of neuron-specific AAV1/2-gene delivery (here, GFP) following injections into L3-L4 DRGs, shown by the lack of GFP colocalization with markers of nonneuronal cells in the DRG (CD31 for blood vessels, α-Schwann for Schwann cells, GFAP for satellite cells).

(E) Evidence for marked knockdown of Fzd3 expression upon injection of AAV-Fzd3 shRNA virions as compared to injection of AAV-scrambled shRNA virions in the DRG via western blot analysis using β-Tubulin-III expression as a control. Densitometric quantification of three independent experiments is shown on the bottom.

(F) Complete blockade of Wnt3a-induced mechanical hypersensitivity in mice injected with AAV-Fzd3 shRNA virions as compared to mice injected with AAV-scrambled shRNA virions in the DRG (n = 7 mice/group).

(G and H) Mice injected with AAV-Fzd3 shRNA virions (G; n = 8 mice) or lentiviral Fzd3 shRNA (H; n = 9 mice) in the DRG develop tumor-associated mechanical hypersensitivity to a markedly lower magnitude than mice injected with AAV-scrambled shRNA (G; n = 8 mice) lentiviral-scrambled shRNA (H; n = 7 mice); *$p < 0.05$ as compared to corresponding control, two-way ANOVA followed by post hoc Fischer's test.

(I) Analysis of tumor area (represented as a fraction of total paw area) did not reveal significant differences in tumor growth between groups tested. Data represent mean ± SEM. See also Figure S8 and Table S5.

interplay between diverse noncanonical Wnt signaling mediators, which, in turn, impact on classical transducers and amplifiers of sensory stimuli. Finally, this study provides evidence for a translational potential for targeting peripheral Wnt signaling in tumor-nerve interactions and pathological pain hypersensitivity, paving the way for therapeutic interventions.

EXPERIMENTAL PROCEDURES

Wild-Type and Transgenic Mice

Nociceptor- or DRG-specific knockout mutants for β-catenin were generated by mating homozygous C57BL/6J mice carrying the floxed alleles for the mouse *Ctnnb1* locus encoding β-catenin (β-catenin$^{fl/fl}$) mice (Huelsken et al., 2001) and either SNS-Cre mice (Agarwal et al., 2004) or Advillin-Cre mice (Zurborg et al., 2011). Details on the above as well as on transgenic mouse lines that have been previously reported are described under the Supplemental Experimental Procedures online materials.

Behavioral Measurements and Transgenic Mice

All animal usage procedures were in accordance with ethical guidelines laid down by the local governing body (Regierungspräsidium Karlsruhe). All behavioral measurements were done in awake, unrestrained, age-matched adult (more than 2 months old) mice. Mice were habituated to the experimental setup in at least two separate sessions within the week preceding the time of behavioral testing. The observer was fully blinded to the identity of the groups in all behavioral tests. See Supplemental Experimental Procedures for details on behavioral tests.

Mouse Models of Tumor-Associated Pain

The bone metastases-pain model as well as the cancer pain model associated with subcutaneous injection of LL2 cells were employed as described previously (Cain et al., 2001; Stösser et al., 2010). See Supplemental Experimental Procedures for details.

Antibodies

The following antibodies were used in this study.

For immunohistochemistry, the antibodies used were anti-Fzd1 (1:100 R&D Systems); anti-Fzd3 (1:400 R&D Systems); anti-phospho-CaMKIIα (1:500; Promega); anti-phospho-Src (1:50; Cell Signaling); anti-phospho-JNK (1:100; Cell Signaling); anti-β-Tubulin III antibody (1:1,000, Sigma); anti-CGRP antibody (1:2,000; Immunostar); anti-NF200 antibody (1:300, Sigma); anti-PGP9.5 antibody (1:500, rabbit polyclonal antibody RA95101; Ultraclone); anti-CD31 antibody (1:200 BD); anti-Schwann antibody (1:10,000, Cosmo Bio); anti-GFAP antibody (1:1,000, Sigma).

For immunofluorescence on cultured cells, the antibodies used were anti-phospho-CaMKIIα (1:500 Promega), anti-phospho-Src (1:50; Cell Signaling), anti-phospho-JNK (mouse anti-pJNK 1:200; Cell Signaling or Rabbit anti pJNK 1:100 Cell Signaling), anti-Fzd3 (1: 400; rat monoclonal R&D Systems), anti-Fzd1 (1:200; R&D System), anti-TRPV1 (1:500 Santa Cruz P-19), anti-β-catenin (1: 50; BD), anti-β-tubulin III (1:1,000; T2200 Sigma) and secondary antibodies conjugated with Alexa 488 or Alexa 594 (Molecular Probes, Invitrogen), anti-myc antibody (1:500; Origene), and anti-Fzd3 (1:400; rat monoclonal, R&D Systems).

For western blotting, the antibodies used were anti-phospho-CaMKIIα (1:700 Promega), anti-phospho-Src (1:1,000; Cell Signaling), anti-phospho-JNK (1:1,000; Cell Signaling), anti-Src (1:700; Cell Signaling), anti-Wnt3a (1:700; R&D System), anti-Wnt5a (biotinylated antibody 1:1,000; R&D System), anti-β-tubulin (1:6,000, T2200, Sigma Aldrich), anti-GAPDH (1:500; Santa Cruz, an anti-TRPV1 antibody (goat P-19 1:500, Santa Cruz), or with an anti-TRPV1 antibody kindly provided by D. Julius (UCSF).

For lentiviral or AAV virions injection into the DRG, the antibodies used were AAV-Fzd3-shRNA-GFP (VectorBiolabs) or control AAV-shRNA scramble GFP plasmid and AAV-Rac1 shRNA (IBA), AAV-CRE or AAV-GFP plasmid were used to produce AAV-virions. Lentiviral or AAV injections into the DRGs in vivo were performed as described in details previously (Schweizerhof et al., 2009).

Gene Profiling

DRG cultures were serum starved for 1 hr and then treated with Wnt3a (200 ng/ml) or vehicle (PBS) for 6 hr. Total RNA was extracted with Trizol (Life Technologies) followed by clean-up and DNase I treatment with QIAGEN RNeasy mini kit in accordance with the prescribed protocol provided with the kit. RNA quality control was performed with Agilent Bioanalyzer. Microarray profiling was performed at the Genomics and Proteomics Core Facility of the German Cancer Research Center (DKFZ) using Illumina Sentrix expression BeadChips (mouseRef-8 v2) according to the manufacturer's recommendations. The microarray data were deposited in the GEO database (http://www.ncbi.nlm.nih.gov/geo/) under accession number GSE56880. See Supplemental Experimental Procedures for details.

Statistics

All data are expressed as mean ± SEM. Two-way ANOVA followed by post hoc Fisher's tests were used to assess statistical significance. Changes with $p < 0.05$ were considered to be significant.

Additional methods are described under Supplemental Experimental Procedures.

ACCESSION NUMBERS

The GEO accession number for the microarray data reported in this paper is GSE56880.

SUPPLEMENTAL INFORMATION

Supplemental Information includes Supplemental Experimental Procedures, eight figures, and five tables and can be found with this article online at http://dx.doi.org/10.1016/j.neuron.2014.05.037.

ACKNOWLEDGMENTS

The authors thank Rose LeFaucheur for secretarial help, Hans-Joseph Wrede, Karin Meyer, Nadine Gehrig, and Dunja Baumgartner-Ahlert for technical assistance. The authors thank Stefano Piccolo, University of Padua, Italy for kindly providing BAT-GAL mice and David Julius, UCSF, USA for generously providing the TRPV1 antibody. The authors acknowledge core facilities of the University and the DKFZ Heidelberg for their microarray and sequencing services. This work was supported by grants from the Association of International Cancer Research and an ERC advanced Investigator grant 294293 from the European Research Council (ERC) to R.K. R.K. is a principal investigator in the Excellence Cluster CellNetworks of Heidelberg University and M.S. was supported by the CellNetworks Postdoctoral Fellowship program.

Accepted: May 19, 2014
Published: July 2, 2014

REFERENCES

Agarwal, N., Offermanns, S., and Kuner, R. (2004). Conditional gene deletion in primary nociceptive neurons of trigeminal ganglia and dorsal root ganglia. Genesis *38*, 122–129.

Alfaro, M.P., Pagni, M., Vincent, A., Atkinson, J., Hill, M.F., Cates, J., Davidson, J.M., Rottman, J., Lee, E., and Young, P.P. (2008). The Wnt modulator sFRP2 enhances mesenchymal stem cell engraftment, granulation tissue formation and myocardial repair. Proc. Natl. Acad. Sci. USA *105*, 18366–18371.

Basbaum, A.I., Bautista, D.M., Scherrer, G., and Julius, D. (2009). Cellular and molecular mechanisms of pain. Cell *139*, 267–284.

Budnik, V., and Salinas, P.C. (2011). Wnt signaling during synaptic development and plasticity. Curr. Opin. Neurobiol. *21*, 151–159.

Cain, D.M., Wacnik, P.W., Turner, M., Wendelschafer-Crabb, G., Kennedy, W.R., Wilcox, G.L., and Simone, D.A. (2001). Functional interactions between tumor and peripheral nerve: changes in excitability and morphology of primary afferent fibers in a murine model of cancer pain. J. Neurosci. *21*, 9367–9376.

Cavanaugh, D.J., Lee, H., Lo, L., Shields, S.D., Zylka, M.J., Basbaum, A.I., and Anderson, D.J. (2009). Distinct subsets of unmyelinated primary sensory fibers mediate behavioral responses to noxious thermal and mechanical stimuli. Proc. Natl. Acad. Sci. USA *106*, 9075–9080.

Durand, J., Lampron, A., Mazzuco, T.L., Chapman, A., and Bourdeau, I. (2011). Characterization of differential gene expression in adrenocortical tumors harboring beta-catenin (CTNNB1) mutations. J. Clin. Endocrinol. Metab. *96*, E1206–E1211.

Fodde, R., and Brabletz, T. (2007). Wnt/beta-catenin signaling in cancer stemness and malignant behavior. Curr. Opin. Cell Biol. *19*, 150–158.

Glinka, A., Wu, W., Delius, H., Monaghan, A.P., Blumenstock, C., and Niehrs, C. (1998). Dickkopf-1 is a member of a new family of secreted proteins and functions in head induction. Nature *391*, 357–362.

Grigoryan, T., Wend, P., Klaus, A., and Birchmeier, W. (2008). Deciphering the function of canonical Wnt signals in development and disease: conditional loss- and gain-of-function mutations of beta-catenin in mice. Genes Dev. *22*, 2308–2341.

Hartmann, B., Ahmadi, S., Heppenstall, P.A., Lewin, G.R., Schott, C., Borchardt, T., Seeburg, P.H., Zeilhofer, H.U., Sprengel, R., and Kuner, R. (2004). The AMPA receptor subunits GluR-A and GluR-B reciprocally modulate spinal synaptic plasticity and inflammatory pain. Neuron *44*, 637–650.

Huelsken, J., Vogel, R., Erdmann, B., Cotsarelis, G., and Birchmeier, W. (2001). beta-Catenin controls hair follicle morphogenesis and stem cell differentiation in the skin. Cell *105*, 533–545.

Ishitani, T., Kishida, S., Hyodo-Miura, J., Ueno, N., Yasuda, J., Waterman, M., Shibuya, H., Moon, R.T., Ninomiya-Tsuji, J., and Matsumoto, K. (2003). The TAK1-NLK mitogen-activated protein kinase cascade functions in the Wnt-5a/Ca(2+) pathway to antagonize Wnt/beta-catenin signaling. Mol. Cell. Biol. *23*, 131–139.

Kaan, T.K., Yip, P.K., Patel, S., Davies, M., Marchand, F., Cockayne, D.A., Nunn, P.A., Dickenson, A.H., Ford, A.P., Zhong, Y., et al. (2010). Systemic blockade of P2X3 and P2X2/3 receptors attenuates bone cancer pain behaviour in rats. Brain *133*, 2549–2564.

Kawano, Y., and Kypta, R. (2003). Secreted antagonists of the Wnt signalling pathway. J. Cell Sci. *116*, 2627–2634.

Koltzenburg, M., Stucky, C.L., and Lewin, G.R. (1997). Receptive properties of mouse sensory neurons innervating hairy skin. J. Neurophysiol. *78*, 1841–1850.

Komekado, H., Yamamoto, H., Chiba, T., and Kikuchi, A. (2007). Glycosylation and palmitoylation of Wnt-3a are coupled to produce an active form **of** Wnt-3a. Genes Cells *12*, 521–534.

Komiya, Y., and Habas, R. (2008). Wnt signal transduction pathways. Organogenesis *4*, 68–75.

MacDonald, B.T., Tamai, K., and He, X. (2009). Wnt/beta-catenin signaling: components, mechanisms, and diseases. Dev. Cell *17*, 9–26.

Maretto, S., Cordenonsi, M., Dupont, S., Braghetta, P., Broccoli, V., Hassan, A.B., Volpin, D., Bressan, G.M., and Piccolo, S. (2003). Mapping Wnt/beta-catenin signaling during mouse development and in colorectal tumors. Proc. Natl. Acad. Sci. USA *100*, 3299–3304.

Mikels, A.J., and Nusse, R. (2006). Purified Wnt5a protein activates or inhibits beta-catenin-TCF signaling depending on receptor context. PLoS Biol. *4*, e115.

Niehrs, C. (2006). Function and biological roles of the Dickkopf family of Wnt modulators. Oncogene *25*, 7469–7481.

Patapoutian, A., and Reichardt, L.F. (2000). Roles of Wnt proteins in neural development and maintenance. Curr. Opin. Neurobiol. *10*, 392–399.

Petrus, M., Peier, A.M., Bandell, M., Hwang, S.W., Huynh, T., Olney, N., Jegla, T., and Patapoutian, A. (2007). A role of TRPA1 in mechanical hyperalgesia is revealed by pharmacological inhibition. Mol. Pain *3*, 40.

Schweizerhof, M., Stösser, S., Kurejova, M., Njoo, C., Gangadharan, V., Agarwal, N., Schmelz, M., Bali, K.K., Michalski, C.W., Brugger, S., et al. (2009). Hematopoietic colony-stimulating factors mediate tumor-nerve interactions and bone cancer pain. Nat. Med. *15*, 802–807.

Shan, J., Shi, D.L., Wang, J., and Zheng, J. (2005). Identification of a specific inhibitor of the dishevelled PDZ domain. Biochemistry *44*, 15495–15503.

Stösser, S., Agarwal, N., Tappe-Theodor, A., Yanagisawa, M., and Kuner, R. (2010). Dissecting the functional significance of endothelin A receptors in peripheral nociceptors in vivo via conditional gene deletion. Pain *148*, 206–214.

Tsuda, M., Koizumi, S., Kita, A., Shigemoto, Y., Ueno, S., and Inoue, K. (2000). Mechanical allodynia caused by intraplantar injection of P2X receptor agonist in rats: involvement of heteromeric P2X2/3 receptor signaling in capsaicin-insensitive primary afferent neurons. J. Neurosci. *20*, RC90.

Yuan, S., Shi, Y., and Tang, S.J. (2012). Wnt signaling in the pathogenesis of multiple sclerosis-associated chronic pain. J. Neuroimmune Pharmacol. *7*, 904–913, http://dx.doi.org/10.1007/s11481-012-9370-3.

Zhang, X., Huang, J., and McNaughton, P.A. (2005). NGF rapidly increases membrane expression of TRPV1 heat-gated ion channels. EMBO J. *24*, 4211–4223.

Zhang, Y.K., Huang, Z.J., Liu, S., Liu, Y.P., Song, A.A., and Song, X.J. (2013). WNT signaling underlies the pathogenesis of neuropathic pain in rodents. J. Clin. Invest. *123*, 2268–2286.

Zurborg, S., Piszczek, A., Martínez, C., Hublitz, P., Al Banchaabouchi, M., Moreira, P., Perlas, E., and Heppenstall, P.A. (2011). Generation and characterization of an Advillin-Cre driver mouse line. Mol. Pain *7*, 66.